HIGH PRESSURE GRINDING ROLLS MODELLING WITH POPULATION BALANCE MODELS APPLIED TO TANTALUM ORE

Hernan Anticoi, Eduard Guasch, Sarbast A. Hamid, Josep Oliva, Pura Alfonso, Teresa Escobet.
Departament d'Enginyeria Minera, Industrial i TIC, Universitat Politècnica de Catalunya Barcelona Tech,
Av. Bases de Manresa 61-63, Manresa (08242) Barcelona, Spain
eduard.guasch@emrn.upc.edu

Abstract

High pressure grinding rolls are a good alternative for comminution. This device presents low operative cost and high energy performance. Modelling of 16 mono-size assays have been carried out using grinding rolls with controlled operative pressure and tangential velocity. Back-calculation of the different parameters of the model have been developed with MATLAB software. The fitting of the simulated curve is in a good agreement with the experimental data in a wide range of tests. The present model describes correctly the physical behaviour of the particles within the high pressure grinding roll. The error is low except for experiments with small feed particle size. This situation could be explained because for fine particle sizes the bed compression phenomenon is predominant. The particle size distribution has been monitored in the input and output for each assay. The validation experiments show that the model is consistent. The selection function describes adequately the breakage probability of the particles inside the high pressure grinding rolls. Then, the present model is a good alternative for simulating a high pressure grinding roll process.

Keywords

High Pressure Grinding Rolls, Grinding, Modelling.

1. Introduction

High pressure grinding rolls is a modern technology that is proven to reduce the operating costs in full scale plants when compared with other milling technologies, especially with low grades ores and inherent low efficiency of the conventional comminution system (Abouzeid and Fuerstenau, 2009). These devices offers benefits on energy saving and simplicity in the process; however, the particle size reduction is less than with other types of comminution devices, as the ball mill. In addition high pressure grinding rolls produce much more internal particle fractures than other devices (Fernandez and Brochot, 2014). These equipments have been studied and applied, first in the cement clinker industry (Kellerwessel, 1990; Hasanzadeh and Farzanegan, 2011) and after in mining activities, especially in metallic ore deposits (Austin et al, 1991; Guevara and Menacho, 1992; Morrel et al, 1997; Torres and Casali 2009; Abouzeid and Fuerstenau, 2009; Saramak, 2011; Numbi and Xia, 2015). Whereas in conventional crushers the impact and abrasion breakage mechanism are dominant in the high pressure grinding rolls the particles are broken by compression in a packed particle bed, and not by direct nipping of the particles between the two rolls (Ghorbani et al., 2013).

The High Pressure Grinding Rolls modelling can be structured in three main parts; (a) throughput modelling, (b) Power and energy model and (c) particle size distribution modelling (Austin et al, 1991; Guevara and Menacho, 1992; Austin and Trubelja, 1994; Morrel et al, 1997; Torres and Casali, 2009).

Guevara and Menacho (1992) follow several hypothesis about throughput modelling; (a) null displacement between the mineral and the roll in the zone where the pressure reach the maximum value, (b) shear stress over the rolls are governed by Coulomb equation, (c) the internal stress in the bed compression zone does not vary through the length of the rolls.

Austin et al (1993) indicate that the total force measured is the integral of the horizontal compressive forces up to the gap. The specific grinding pressure is expressed in geometric terms of the device. This pressure increases and reaches a maximum compression effect at the gap, leading to a higher bulk density of material passing through the gap. However, a smaller gap means that the separation of the roller at some critical nip angle is lower, so the throughput decreases with the specific grinding pressure. Morrel et al (1997) as well as Austin, indicate that the variation of the throughput is a linear logarithmic function of the specific grinding force, the rolls speed and the gap. Torres and Casali (2009) refers that under steady state conditions the difference of tonnage between the beginning and the end of the particle bed compression zone is equal to zero, then the throughput can be calculated in function of the geometry of the device, the gap and the apparent density of the ore before enter to the nip angle influence and the apparent density in the extrusion zone.

For the power and energy model, the authors specially refer to the energy consumed by the pressure to the rolls as the specific power draw (Guevara and Menacho, 1992) or as the power required by the high pressure grinding rolls at the rolls in terms of the torque and the angular velocity (Morrell et al, 1997). Torres and Casali (2009) indicated that this device is operated in a choke fed condition, so the applied pressure is distributed only in the upper right half of the roll. The power draw is function of the specific pressure, diameter of the roll, the nip angle and the tangential speed of the rolls.

For determining the produced particle size distribution, Population Balance Model is mainly used (Dundar et al., 2013). The simplest case is the Guevara and Menacho model, expressing the product in terms of the kinetic function, the specific energy and the feed in cumulative percentage. In many cases, the comminution is based in the studies on grinding rolls devices and considers two distinctly different ways; first, a single particle compression or pre-crushing zone (Morrell et al, 1997; Torres and Casali, 2009) where the particles break slowly with the simple contact to the rolls under pure compression (Fuesternau et al, 1991). Then, a bed compression zone is defined as a place where the product of the single particle compression form a bed of particle and comminution occurs primarily by very high localized inter-particle stresses generated within the particle bed, due to the contact to the rolls. The piston flow arrangement is produced, because the pressure increase considerably by the lessening of volume as the material approaches to the gap (Fuesternau et al, 1991; Torres and Casali, 2009). It is important to mention that the author distinguish between the particles that are broken by simple compression, but other material bypass without breakage. These particles joint to the product of the single particle compression for forming the bed particle compression zone (Austin et al, 1991; Torres and Casali, 2009; Kwon et al, 2012). Schneider et al (2009) incorporated the specific grinding pressure into the Austin's population balance model and

took into account the increase of the gap during grinding test for determining the product. Furthermore, two different breakage functions were recommended to use; Austin's function and the truncated Rosin-Rambler breakage function, and depending of the ore type, one of them or both can be used to predict the particle size distribution product. Torres and Casali (2009), for modelling the particle size distribution, consider a discretization of N_B blocks through the rolls length where each one have a particular compression force, power consumption and rate of breakage.

The aim of this study is to show a new population balance model and the adjustment of the parameters for Tantalum ore applied to high pressure grinding rolls to improve the physical description of the process and allow better adjustments for this material.

2. Materials and methods

The tested material was a low grade tantalum-rich altered leucogranite from the Penouta Open Pit Mine, Northwest of Spain. Leucogranite is mainly composed of quartz, muscovite, K-feldspar and albite. It is highly altered and kaolinite is present. The ore is mainly constituted by cassiterite and columbite group minerals. About 250 kg of material were sampled and used for the experiments. The sample was crushed by a KHD Humblot Wedag jaw crusher, screened and classified by size classes from -19 +16 mm, -16 +14 mm, -14 +12.5 mm, -12.5 +11.5 mm, -11.5 +9.5 mm, -9.5 +8 mm, -8 +6.7 mm and -6.7 +5 mm mesh in order to perform mono-size experiments.

A total of 16 tests were performed with a KHD Humblot Wedag smooth roll crusher with controlled pressure and an engine of 3 kW. The dimensions of the rolls are 250 mm in diameter and 150 mm in width but only 50 mm are used in this work. The gap setting from 0 to 7 mm. Pressure was controlled by means of a hydraulic system incorporated to the device with two 60 mm internal diameter pistons. Three gap configurations were used, 3 mm, 4 mm and 5 mm. In order to observe the mechanical behaviour of the material, a transparent cover was used and was captured with a slow motion camera. The horizontal movement and the speed of the rolls was monitored.

Methodology is divided in four different stages: (1) Preparation of the materials and determination of operative parameters, (2) Selection of the model and experiments execution, (3) modelling and back-calculation for finding the different parameters of the function for breakage and selection function and (4) validation of the parameters with specific experiments. The calculated parameters from several assays were used to simulate and validate the model.

The operative parameters were controlled for each test (Table 1). Bulk density of the material was measured at both the inlet and outlet. The flow was determinated with the total mass and the time of each assay. The product particle size distribution was determined. For parameter adjusment, MATLAB software and backcalculation *globalsearch* solver was used.

Table 1. Operative parameters of representative tests.

Parameters	Units		M-1	M-2	M-3	M-4	M-5	M-6	M-7	M-8	M-9	M-10	M-11	M-12	M-13	M-V1	M-V2	M-V3
Bulk density (inlet)	t/m³	ρ	0.86	0.83	1.07	1.12	1.07	1.09	1.16	0.86	1.07	1.12	1.09	1.16	0.83	0.86	0.83	1.12
Bulk density (outlet)	t/m³	δ	1.57	1.46	1.48	1.47	1.48	1.57	1.54	1.57	1.48	1.47	1.57	1.54	1.46	1.57	1.46	1.47
Tangential velocity	m/s	U	1.0	1.0	1.0	1.0	0.7	0.7	0.7	0.4	0.6	0.7	0.7	0.6	0.7	0.8	0.7	0.7
Velocity	rpm	v	76	76	76	76	53	53	53	30	45	53	53	45	53	61	53	53
Pressure	MPa	Po	10	10	10	10	10	10	10	8	8	8.5	8.5	8.5	8.5	10	10	10
Force	kN	F	490	490	490	490	490	490	490	390	390	417	417	417	417	490	490	490
Flow	t/h	G	1.2	1.3	1.2	1.4	1.0	1.3	1.3	1.2	0.8	1.2	1.0	1.3	1.1	1.0	0.9	1.1
Gap	mm	S_0	5	5	5	5	5	3	3	3	3	3	3	3	3	5	5	5
Feed particle mono-size	mm		-19 +16	-16 +14	-14 +12.5	-12.5 +11.5	-12.5 +11.5	-9.5 +6.7	-6.7 +5	-19 +16	-12.5 +11.5	-14 +12.5	-9.5 +6.7	-6.7 +5	-16 +14	-19 +16	-16 +14	-14 +12.5

3. Modelling

In the present work the motion of the particles are described by Newtonian physics in a steady mass-balance of the material passing through the rolls (Torres and Casali, 2009). In addition, the breakage can be described in several steps and the relationship with a selection function, including parameters dependent on the geometry of the device and the material mechanical characteristics (Austin, 1993; Austin and Trubelja, 1994). This study departs from the hypothesis that the comminution for particles bigger than the gap can be expressed as a dual process, with an initial stage where the single particle compression phase for the oversize particles and then, during the second stage, a bed of particles is formed, producing the particle bed compression phase. Figure 1 shows a schematically formulation of the process, where the single particle compression is divided in three stages according to the evolution of the rolls separation and the particle size is regulated with the selection function. In the second step the behavior can be described as a particle bed compression.

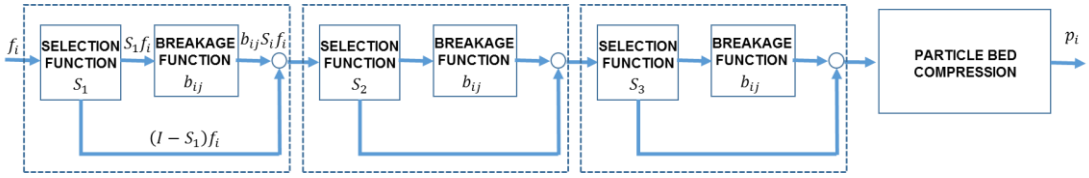

Figure 1. Scheme of the proposed population balance model for high pressure grinding rolls.

The selection function from Whiten et al. (1979) mainly used for cone crushers, also applicable to roll crushers and high pressure grinding rolls (Equation 1) describes adequately this physical process in the steps where the single particle compression occurs. This function has the particularity of fixing upper and under edges, related to the device geometry and the mineral characteristics.

$$S_n = 1 - \left(\frac{dp - x_n}{d_1 - x_n}\right)^{\gamma} \qquad for\ d_1 < dp < x_n \tag{1}$$

$$S_n = 0 \qquad for\ dp < d_1$$

$$S_n = 1 \qquad for\ dp > x_n$$

where, the upper limit x_n is given by the distance between the rolls when the nipping action begins, the under limit d_1 represents those particles that cannot be retained in the comminution zone due to their size that slip through the larger particles and the parameter γ can be related to mineral characteristics and describes the behaviour of the curve. For the breakage function, the standard form presented by Whiten et al. (1979) is used in equation 2.

$$B_{ij} = k\left(\frac{x}{y}\right)^{n_1} + (1-k)\left(\frac{x}{y}\right)^{n_2} \tag{2}$$

where k, n_1 and n_2 are the parameters of the model.

The mathematical relation of the distance between the rolls and the compression angle is shown in Equation 3.

$$x_n(\alpha) = S_0 + D(1 - \cos\alpha) \tag{3}$$

The throughput model (Torres and Casali 2009) presents the methodology for compression angle calculation (Equations 4, 5, 6 and 7), in terms of change of the bulk density through the rolls, maintaining the flow as constant (Fig. 2).

$$cos(\alpha) = \frac{1}{D}\left[(S_0 + D) + \sqrt{(S_0 + D)^2 - \frac{4S_0\delta D}{\rho_a}}\right] \quad (4)$$

$$G_S(\alpha) = 3600\ \delta\ S_0\ L\ U \quad (5)$$

$$z = \frac{D}{2}\sin(\alpha_{NIP}) \quad (6)$$

$$v_z = U\cos(\alpha_{NIP}) \quad (7)$$

where $\rho(\alpha_{nip})=\rho_a$ (t/m^3) is the bulk density at the feed zone, $\rho(0)=\delta$ (t/m^3) the bulk density at the extrusion zone, L (m) the roll length, U (m/s) the tangential velocity, G_S (t/h) the throughput, D (m) is the diameter, S_0 (m) is the gap, z is the vertical distance between the gap and where the nipping is produced and v_z is the velocity of the bulk through the rolls.

For the particle bed compression zone, the comminution is described by the Equation (8):

$$v_z\ \frac{dp_i}{dz} = \sum_{j=1}^{i-1} k_{i,j}\ b_{i,j}\ p_j - k_i\ p_i \quad (8)$$

where this equation is solved for each size class *i* (*i*=1,……,N). The rate of breakage is defined as $k_{i,k}$. b_{ij} is the breakage function, v_z is the velocity of the particles in the vertical or flow direction (z), p_i and p_j are the differential mass of the feed and the product, respectively.

The equation 6 is similar to the batch grinding kinetic equation, which has been solved analytically (Reid 1965). The boundary conditions for solving the equation (8) are described below (9) and (10).

$$p_i(z = 0) = p_i^F \quad (9)$$

$$p_i(z = L) = p_i^P \quad (10)$$

The system solution for the N size classes is written as follows (11), (12):

$$p_i^P = \sum_{j=1}^{i} A_{ij}\ exp\left(-\frac{k_j}{v_z}\ v_z\right) \quad (11)$$

$$A_{ij} = \begin{cases} 0 & i < j \\ \sum_{l=j}^{i-1} \frac{b_{il}\ k_l}{k_i - k_j} A_{lj} & i > j \\ p_i^F - \sum_{l=1}^{i-1} A_{il} & i = j \end{cases} \quad (12)$$

For the breakage rate, the functional expression (Herbst and Fuerstenau, 1980) presented in Eq. (13) is used. The advantage of using this expression lies on the scale up relationship among the specific rate of breakage, S_i^E ; invariant, and the quotient between Power, P and Holdup, H, as it is shown in Eq. (14), Eq. (15) and Eq. (16).

$$\ln\left(\frac{S_i^E}{S_1^E}\right) = \zeta_1 \ln\left(\frac{x_i}{x_1}\right) + \zeta_2 \left(\ln\left(\frac{x_i}{x_1}\right)\right)^2 \quad (13)$$

$$k_i = \frac{P}{H} S_i^E \quad (14)$$

$$H = \frac{Gs}{U} z \quad (15)$$

$$P = 2Fsin(\frac{\alpha_{nip}}{2}) \quad (16)$$

where ζ_1, ζ_2 and S_1^E are model parameters to be adjusted with the experimental data.

4. Results and discussion

Experimental observations suggest that for a certain angle, mainly the half of nip angle, the single particle compression goes to the piston flow phenomena. In this stage, a bed formed by multiple fine size fraction particles is observed. The oversize particles have been broken in the three previous stages. For simplify the mathematical discretization, from the upper half of the distance between the gap and where the nipping effect begins, three critical equidistances between the rolls were selected (Fig. 2).

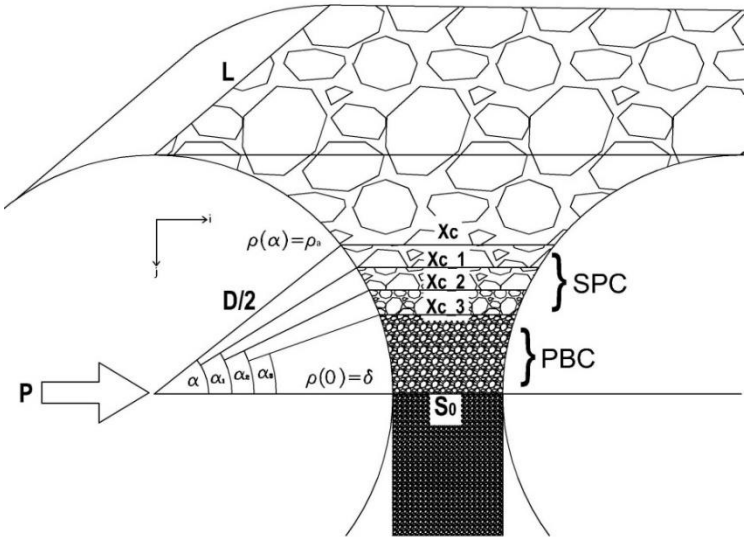

Figure 2. Description of the device geometry showing the different discretized zones for the single particle compression (SPC) with three different angles, and the particle bed compression (PBC), being S_0, Xc, Xc_1, Xc_2 and Xc_3 different distance between the rolls for different angles from the centre of each roll.

Figure 3 shows all the results of the thirteen experiments developed. Experimental values and simulated curves of all the experiments are plotted. The simulated values are obtained using MATLAB software back-calculation methodology. The fitting of the simulated curve is in a good agreement with the experimental data in a wide range of tests. Thus, the proposed model describes correctly the physical behaviour of the particles within the high pressure grinding roll. Only in the experiments with the smallest feed particle size the fitting is less accurate. This situation could be explained because for fine particle sizes the bed compression phenomenon is predominant. The feed parameter has a direct influence in the reduction of the particle size; similarly as found in other experiments made with recirculation load, where the size decrease as the recirculation load increases (Ozcan et al., 2015).

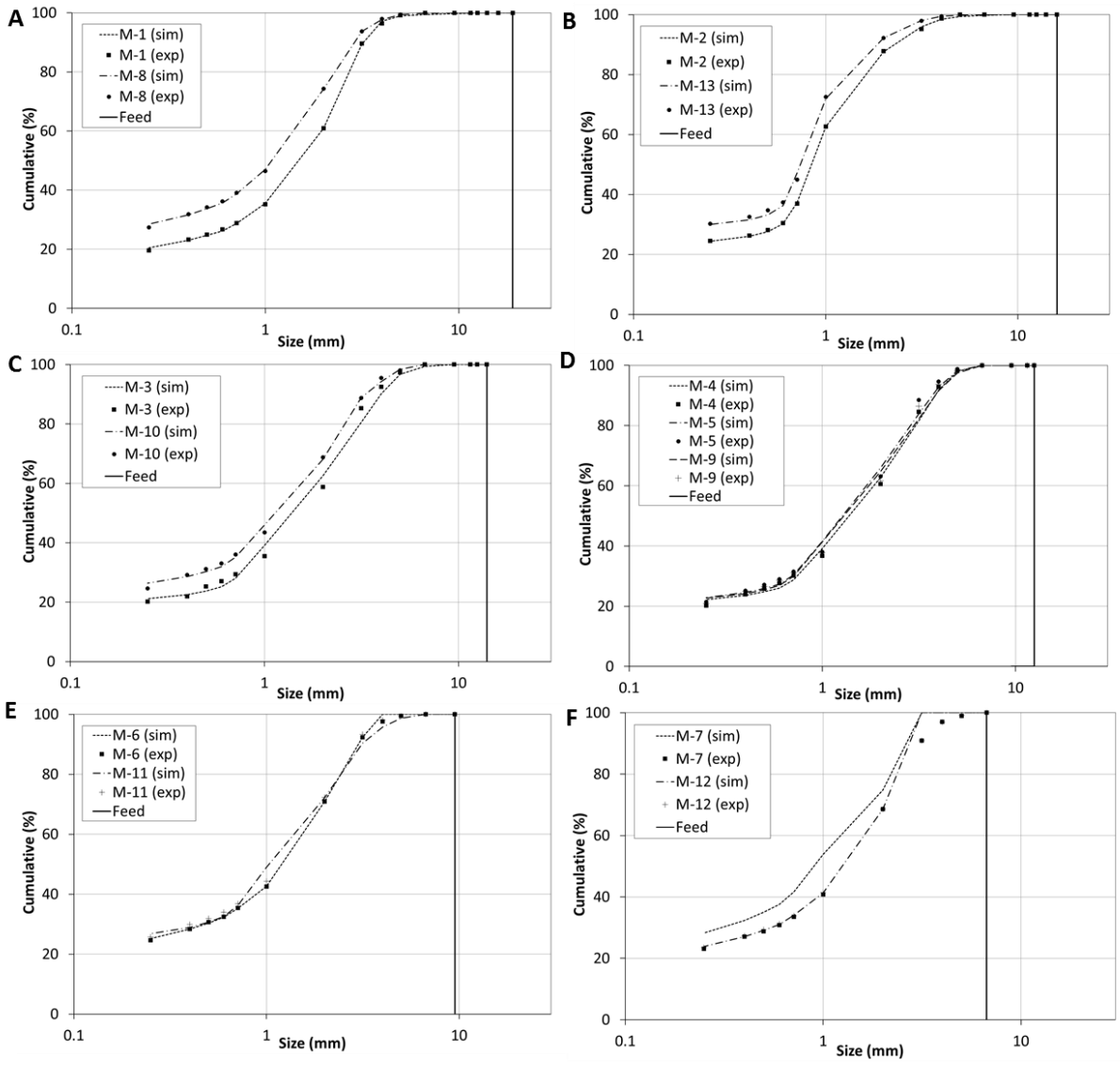

Figure 3. Experimental (exp) and simulated (sim) particle size distributions for all the experiments. (A) to (F) are -19 +16, -16 +14, -14 +12.5, -12.5 +11.5, -9.5 +6.7 and -6.7 +5 mm feed particle sizes respectively.

The results of the back-calculations are in Table 2. The parameters of the process are different in each experiment due to the operation conditions vary among them. The error varies from 0.111 and 1.806, with the exception of the two experiments with smallest feed particle size (M-7 and M-12) where the error is about 7. This error was calculated between the difference of the experimental and simulated date in absolute value.

Table 2. Back-calculated parameters of all the experiments.

Parameters	M-1	M-2	M-3	M-4	M-5	M-6	M-7	M-8	M-9	M-10	M-11	M-12	M-13
k	0.106	0.125	0.139	0.186	0.147	0.240	0.252	0.194	0.190	0.170	0.152	0.257	0.193
n_1	0.349	0.334	0.261	0.347	0.355	0.317	0.350	0.287	0.166	0.335	0.331	0.349	0.317
n_2	12.007	9.416	3.959	5.031	19.471	4.879	7.218	3.955	1.658	13.771	17.651	7.120	5.006
γ	0.666	2.857	2.889	1.351	1.001	2.998	2.547	2.201	0.431	1.303	2.665	1.941	2.304
D_1	0.002	0.002	0.002	0.002	0.002	0.002	0.002	0.002	0.002	0.002	0.002	0.001	0.002
S_1^E	0.197	0.098	13.314	0.001	0.001	2.831	21.531	43.086	0.067	0.006	0.021	3.389	0.069
ζ_1	-4.170	-4.321	3.745	-10.078	-13.833	0.122	3.579	2.806	-8.496	-7.514	-7.022	4.875	-4.416
ζ_2	-2.274	-2.172	0.436	-3.888	-5.042	-1.160	-6.341	-0.299	-5.530	-2.919	-3.039	-0.001	-2.298
Error	0.148	0.147	1.806	0.166	0.111	0.484	6.710	0.602	1.113	0.211	0.072	7.229	0.250

The results of the validation experiments, shown in Figure 4, use the back-calculated parameters from the experiments M-1, M-2 and M-3 to validate three different equivalent experiments. The experimental data fits well with the simulated curve obtained.

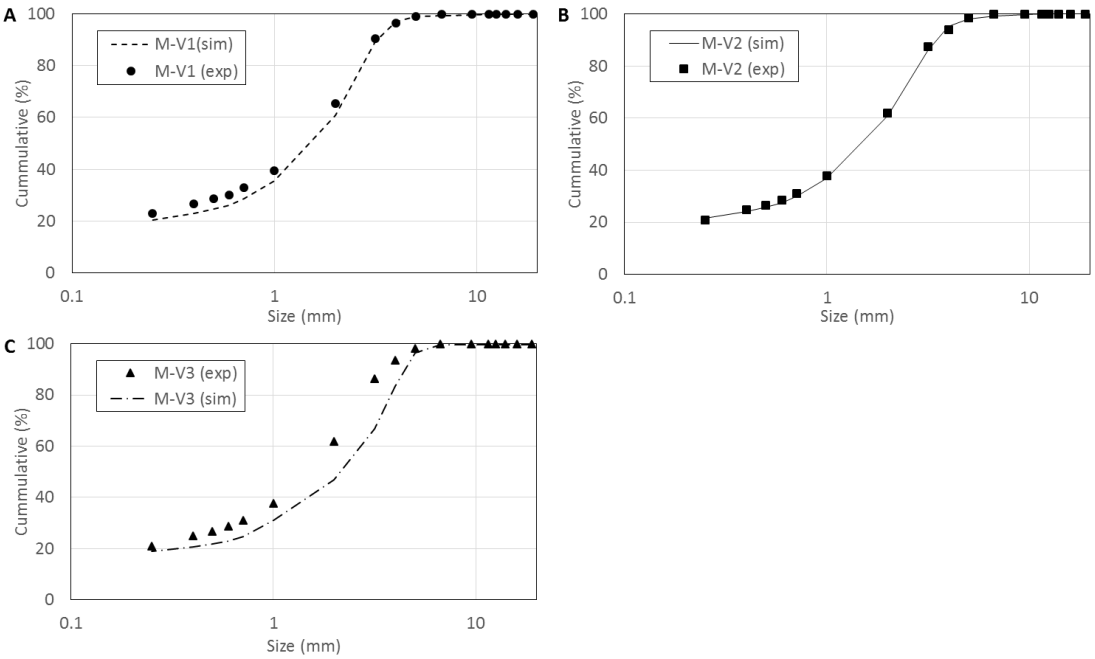

Figure 4. Experimental and predicted curves of the total product mesh size distribution of the assays M-V1 (A), M-V2 (B) and M-V3 (C). The simulated curves were obtained using the back-calculated parameters from the assays M-1, M-2 and M-3 respectively.

The experiment M-V3 could be improved but the numerical error is low. The errors of each experiment M-V1, M-V2 and M-V3 are 0.296, 0.102 and 0.801 respectively.

The single particle compression selection function was simulated in three steps (Fig. 5). The parameters d_1 and γ were back-calculated using MATLAB software and the parameter d_1 shows an average value around 0.0014 m. This result is in accordance with the visual observations. The parameter γ defines the behaviour of the curve between the upper and lower boundaries defined by the parameters x_n and d_1.

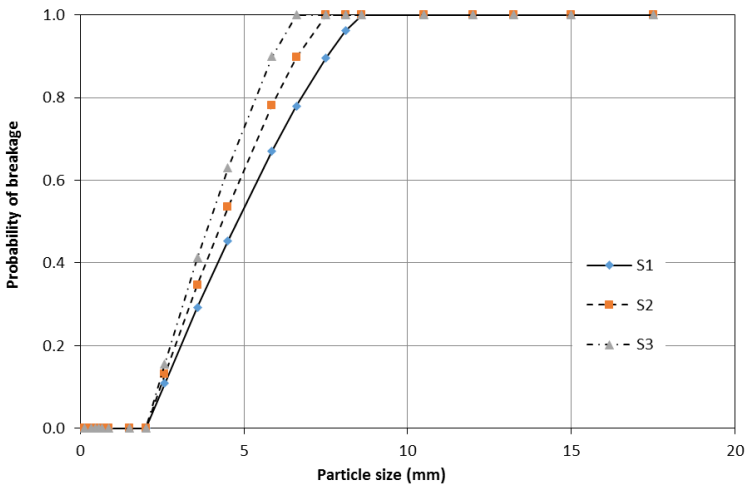

Figure 5. Evolution of the three steps of the selection function for the test M-V2. Particle sizes where all the particles are broken for each step in single compression are 8.6 mm for S1, 7.5 mm for S2 and 6.6 mm for S3.

5. Conclusions

This model is based on a physical description of particles under the comminution action of the high pressure grinding rolls and its main advantage is the good adjustment between the simulations and experimental data, especially in the coarse feed particle sizes. The validation experiments show that the model is consistent.

Although the selection function was developed for cone crushers, it describes adequately the breakage probability of the particles inside the high pressure grinding rolls. In addition, the model present here can be a good alternative for simulating a high pressure grinding roll process.

Acknowledgements

This work is part of the OptimOre project. This project has received funding from the European Union's Horizon 2020 research and innovation programme under grant agreement No 642201. The Strategic Minerals enterprise helped in the sampling of Penouta.

References

Abouzeid, A.-Z.M., Fuerstenau, D.W. (2009). Grinding of mineral mixtures in high-pressure grinding rolls. International journal of mineral processing, 93, 59-65.

Austin, L.G., Trubelja, P.M. (1994). The capacity and product size distribution of high pressure grinding rolls. Mineral Processing and environment.In: Castro, S. and Concha, F. (Eds.), Mineral Processing and Environment. Proceedings of the IV Meeting of the southern hemisphere of mineral technology. 49-67. Universidad de Concepción, Chile.

Austin, L.G., Weller, K.R., Lim, I.L. (1993). Phenomenological Modelling of the High Pressure Grinding Rolls, Proceedings of the XVIII International Mineral Processing Congress, 1, 87-95.

Daniel, M.J., Morrell, S., (2004). HPGR model verification and scale-up. Minerals Engineering 17 (11–12), 1149–1161.

Dundar, H., Benzer, H., Aydogan, N. (2013). Application of population balance model to HPGR crushing. Minerals engineering 50-51,114 -120.

Fernandez, M.G., Brochot, S. (2014). HPGR modelling with mineral liberation for plant optimization. Proceedings of the 27th International Mineral Processing Congress, IMPC 2014, 21-31.

Ghorbani, Y., Mainza, A.N., Petersen, J., Becker, M., Franzidis, J.P., Kalala, J.T. (2013). Investigation of particles with high crack density produced by HPGR and its effect on the redistribution of the particle size fraction in heaps. Minerals Engineering, 43-44, 44-51.

Guevara F., Menacho J., (1993). Modelación mecánica y metalúrgica del molino de rodillos de alta presióon. Centro de lnvestigación Minera y Metalúrgica, Santiago de Chile, 547-563

Hasanzadeh, V., Farzanegan, A. (2011). Robust HPGR model calibration using genetic algorithms. Minerals Engineering 24, 424–432.

Kellerwessel, H., (1990). High pressure material bed comminution in practice. Zement-Kalk-Gips 2, 57–64.

King, R.P., (2001). Modelling and simulation of mineral processing systems. Butterworth-Heinemann, Oxford.

Kwon, J., Cho, H., Mun, M., Kim, K. (2012). Modelling of coal breakage in a double roll crusher considering the reagglomeration phenomena. Powder Technology, 232, 113-123.

Morrel, S., Lim, W., Tondo, L. (1997). Modelling and scale up of the high pressure grinding rolls. In: Proceedings of the. XX International Mineral Congress. IMPC, Aachen, Germany.

Numbi, B.P., Xia, X. (2015). Systems optimization model for energy management of a parallel HPGR crushing process. Applied Energy, 149, 133-147.

Ozcan, O.,Aydogan, N.A.,Benzer, H. (2015). Effect of operational parameters and recycling load on the high pressure grinding rolls (HPGR) performance. International Journal of Mineral Processing 136, 20-25.

Saramak, D. (2011). Technological issues of high-pressure grinding rolls operation in ore comminution processes. Archives of Mining Sciences, 56, 517-526.

Schneider, C., Alves, V., Austin, L. (2009). Modelling the contribution of specific grinding pressure for the calculation of HPGR product size distribution. Minerals Engineering, 22, 642-649.

Torres, M., Casali, A., (2009). A novel approach for the modelling of high-pressure grinding rolls. Minerals Engineering, 22, 1137-1146.

Whiten, W. J., Walter, G. W., White, M. E., (1979). A breakage function suitable for crusher models. 4th Tewkesbury Symposium, Melbourne, pp 19.1-19.3.